

DOI: 10.5281/zenodo.4288263  
CZU 621.9.047



## ELABORATION OF THE PLATFORM FOR FLEXOELECTRIC INVESTIGATION OF GaN MICROTUBES

Elena Monaico<sup>1</sup>, ORCID: 0000-0002-9486-2589,  
Catalin Trifan<sup>1</sup>, ORCID: 0000-0001-6975-7683,  
Eduard Monaico<sup>1</sup>, ORCID: 0000-0003-3293-8645,  
Ion Tiginyanu<sup>1,2</sup>, ORCID: 0000-0003-0893-0854

<sup>1</sup>National Center for Materials Study and Testing, Technical University of Moldova, Bd. Stefan cel Mare 168, Chisinau, MD-2004, Republic of Moldova

<sup>2</sup>Academy of Sciences of Moldova, Bd. Stefan cel Mare 1, Chisinau, MD-2001, Republic of Moldova

\*Corresponding author: Elena Monaico, [elena.monaico@cnstm.utm.md](mailto:elena.monaico@cnstm.utm.md)

Received: 11. 02. 2020

Accepted: 11. 27. 2020

**Abstract.** In this paper, the design and elaboration of a cost-effective technological process for the fabrication of the platform for the study of flexoelectric properties of GaN microtubes with the diameter of 2 - 5  $\mu\text{m}$  and the thickness of the microtube walls of 50 nm is proposed. The impact of the design as well as the electrochemical etching parameters (applied voltage, duration of anodization) on the obtained channel dimensions is investigated. The proposed technological route implies electrochemical etching of n-InP semiconductor crystal in an environmentally friendly electrolyte at high etch rate. The technological process was optimized experimentally. It was proposed to introduce a perpendicular channel in which the microtube will be placed to reach a higher stability on the platform during the measurements.

**Keywords:** *investigation chip, anodization, flexoelectricity, isotropic etching, neutral electrolyte, high etch rate, porous InP.*

### Introduction

In nature there are several types of effects that represent an influence of two phenomena, such as the influence of the magnetic field on a conductor or semiconductor through which electric current flows and as a result the trajectory of the charge carriers changes or uneven heating occurs, depending on the induction magnetic vector (Hall effect and Nernst effect respectively). In addition to these, other effects were discovered, including piezoelectricity, and later flexoelectricity.

Piezoelectricity is an electromechanical effect that consists in applying a uniform mechanical stress to the polarizing sample. This effect was firstly observed in 1880 by Jacques and Pierre Curie when they applied pressure to a quartz crystal and it accumulated electric charge. It should be mentioned that this effect manifests itself in two ways: directly - when applying mechanical stress, the sample/crystal is polarized, and in the opposite way - when applying an electric potential lead to deformation. The materials in which this

mechanism manifests are called piezomaterials and they can be: crystals, ceramics, biological matter, such as bones, DNA and various proteins.

The flexoelectric effect (from the Latin “flexura” - bending) refers to the appearance of electrical polarization in bodies during bending or any other type of non-uniform deformation. This phenomenon is quite common, because, unlike piezoelectricity, it does not imply symmetry restrictions on the choice of material, as long as it is dielectric. Flexoelectricity is observed not only in solids [1 - 3], but also in polymers [4, 5], liquid crystals [6], and biological tissues [7 - 9]. Unfortunately, electric polarization comparable to that obtained at piezoelectric effect cannot be obtained: it is not so easy to create the required gradients of mechanical stress in crystals, and flexible polymers have three orders of magnitude lower values of the flexoelectric effect.

To date, scientifically has been proven that piezoelectricity can exist in 20 out of 32 crystal symmetry classes. At the same time, materials that are able to create electric fields at bending, can belong to absolutely any class of symmetry [10 - 12]. Through slight stretching, the bending of the crystal lattice makes each atomic layer differ from the previous one. Such differences give rise to some changes regarding the placement of ions in the crystal lattice. As a result of such changes, an electric field arises. Due to the fact that intrinsic flexoelectric coefficients tend to be small [13], large deformations are required to achieve substantial flexoelectric responses. Nevertheless, the most increased manifestations of flexoelectricity tend to be found at the nanoscale, where large gradients can be easier achieved [14 - 17].

Nowadays, Si is the most used and popular semiconductor material due to its low cost and availability. Silicon is used for the fabrication of advanced semiconductor structures and devices for micromechanics, optoelectronics and microelectronics. Wet chemical etching in combination with photolithography is a basic process used for spatial shaping of the crystal. The phenomenon of anisotropic wet chemical etching in alkaline solutions has been widely reported in the literature [18 - 22].

However, during the last two decades it was demonstrated that electrochemistry represents not only a cost-effective approach for nanostructuring of semiconductor crystals at high etch rate, but also an environmentally friendly tool due to controlled anodization in salty water [23 - 26]. The purpose of this work is to elaborate a technological platform via an alternative approach based on electrochemical etching in NaCl electrolyte of semiconductor compounds (InP in our case) suitable for flexoelectric investigation of semiconductor microtubes with the wall thickness about several tens of nanometers.

### **The technological process and materials**

In this study crystalline 500- $\mu\text{m}$  thick (100)-oriented substrates of sulfur doped n-InP with the free electron concentration of  $1.2 \times 10^{18} \text{ cm}^{-3}$  were used. The samples were supplied by CrysTec GmbH, Germany. The wafers were cleaned by sonication in acetone for 15 min with subsequent washing in distilled water and drying. The native oxide was removed from the surface by dipping the sample in HCl/H<sub>2</sub>O solution with ratio (1:3) for 2 min. Before the anodization process, conventional photolithography was used to open windows in photoresist covering the top surface of samples. The sample was subjected to the photolithography process, using a positive photoresist (FR) and a strip-shaped mask with a width of 110  $\mu\text{m}$  as well as a space between them of 35  $\mu\text{m}$ . Then the areas not covered with photoresist were subjected to electrochemical etching. The sample with the electrical

contact prepared with silver paste was pressed against an O-ring in a Teflon cell, as shown in Fig. 1, and the surface of 0.2 cm<sup>2</sup> area was exposed to the applied voltage of 5 V for 1 min in 3.5 M NaCl or 5% HCl electrolyte. The anodization was performed in potentiostatic regime at room temperature ( $T = 25\text{ }^{\circ}\text{C}$ ) in three electrode configurations with a Pt mesh with the surface area of 6 cm<sup>2</sup> acting as counterelectrode (CE), a saturated Ag/AgCl reference electrode (RE) and the sample as working electrode (WE). The potentiostat was fully controlled via PC unit. The steering of the electrolyte was provided by Teflon agitator connected to the motor. The rotation speed of 150 r·min<sup>-1</sup> was controlled by applied potential from an external power supply to the motor. The purpose of this step was to create a porous structure with pores large enough to easily destroy the walls between them and to obtain the desired channel. To remove the formed porous regions, the sample was held in HCl:H<sub>3</sub>PO<sub>4</sub> solution with a ratio of 1:1 for 20 seconds. The morphology of the anodized InP samples was investigated using TESCAN Vega TS 5130 MM scanning electron microscope (SEM).

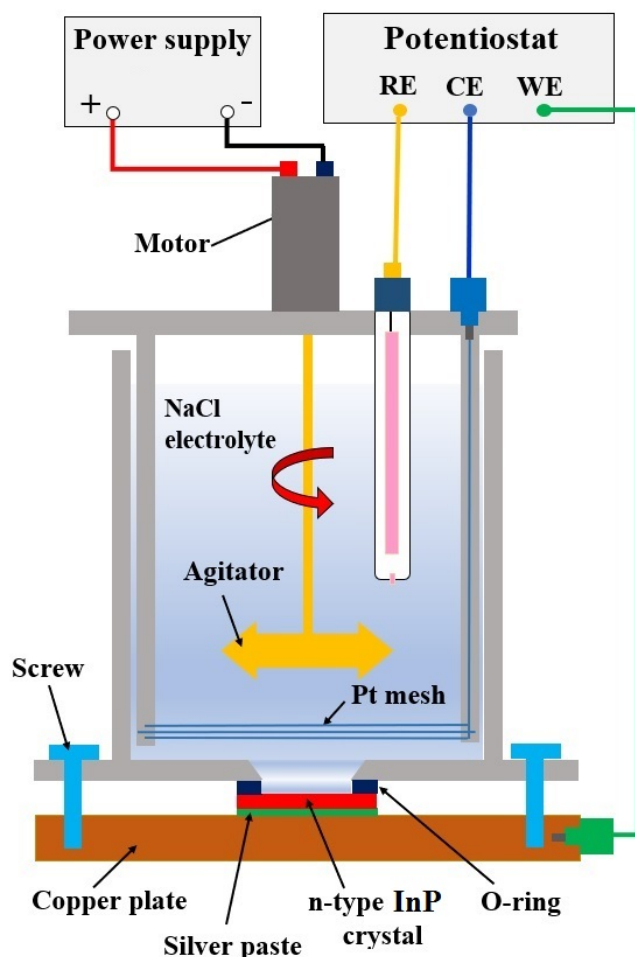


**Figure 1.** Schematic representation of the electrochemical etching setup.

### Optimization of the platform design and technological approach

It is obvious that when force is applied over the sample placed on a flat platform, as is shown in Figure 2a, we will not be able to extract any electrical signal due to the difficulty of creating a mechanical strain gradient and it is not excluded the risk to destroy the wall of the investigated microtube having thickness about 30-50 nm. Therefore, it is necessary to create a space in the platform under the microtube in order to be able to bend

the sample when a force is applied. It is proposed to form a channel under the investigated microtube, as is shown in Figure 2b. The desired channel can be introduced by anisotropic chemical etching of Si substrates with crystallographic orientation (100). Thus, according to Figure 2c, when the mechanical stress is applied, the GaN microtube will have enough space underneath for deformation. However, it should be noted that the given configuration of the “V” type channel is not perfect because the angle formed between the  $\langle 111 \rangle$  direction with the surface of the platform is an angle of 135 degrees, which could prevent the free deformation of the microtube.

In connection with this, it is proposed to modify the cross-section of the channel from „V” shape to semicircle „C”, as is shown in Figure 2d, e. The given configuration of the channel will expose as high angle as to allow bending of the microtube without any impediments.

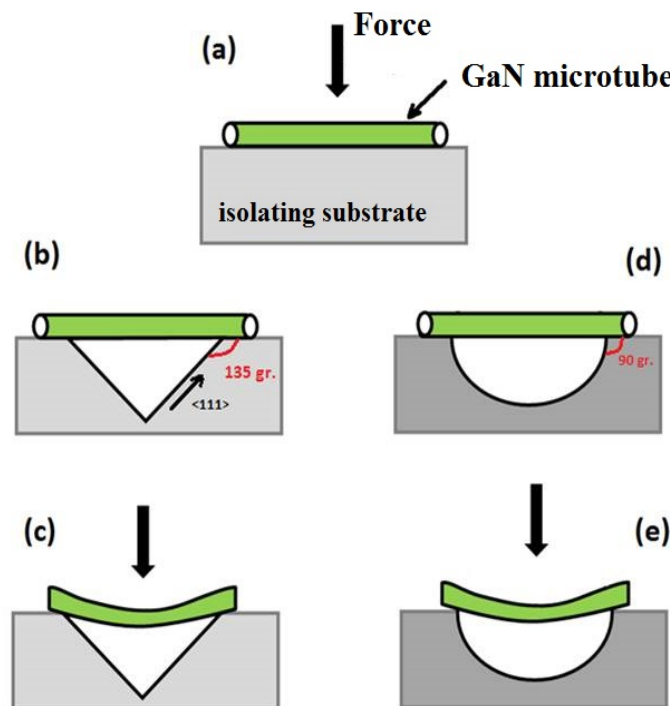


**Figure 2.** Schematic representation of the application of mechanical stress to a tubular sample. The cross-section of the substrate developed with a “V” shaped channel (b, c) and the optimized version with a semicircle “C” channel (d, e).

Both shapes of the channels could be obtained via anisotropic and isotropic wet etching of Si crystals for the V-type channel and semicircle C-type channel respectively [3]. In the anisotropic etching, the etch rate is different for different crystallographic orientations, while isotropic etching is characterized by the same etch rate in all directions. Besides this, acidic and alkaline wet etching have different etch rates that define the anisotropy of the etching. The etch rate of alkaline solutions are generally lower than the etch rates in acidic etching solutions. One important particularity of the anisotropic etching is that alkaline etch processes are often performed at high temperatures (70-80 °C) reaching an etch rate of 1-2  $\mu\text{m}\cdot\text{min}^{-1}$ . The etch rate can be increased to 2-4  $\mu\text{m}\cdot\text{min}^{-1}$  by increasing the concentration of the etchant solution, but the etch mechanism becomes more isotropic. At the same time, acidic etching is performed at low temperatures (6-20 °C) and is normally isotropic reaching etch rates up to 5  $\mu\text{m}/\text{min}$  at 6-10 °C. Taking into

account that usually a KOH based electrolyte is used for anisotropic etching of Si, the inherent low etch rate and elevated temperature of the electrolyte leads to the attack of the photoresist protective layer on the crystal surface.

The could serve as an alternative approach electrochemical etching of semiconductor crystals. It is known that electrochemical etching is a cost-effective process and has a high etch rate [23]. Based on this, it is proposed to form a porous layer in the regions not covered by the photoresist (channel region), then the process is followed by dissolution of formed porous layer in concentrated HCl:H<sub>3</sub>PO<sub>4</sub> electrolyte, as it is described in the experimental section. Then, a dielectric layer from SiO<sub>2</sub> or Si<sub>3</sub>N<sub>4</sub> is deposited on the developed platform to provide short circuit protection of the investigated microtube.

It is known that positioning of the micro-nanoobjects exactly on the channel is challenging. To solve this problem, the optimization of the mask design was proposed. It is proposed to create an array of parallel channels rather than an individual channel. The schematic representation of the main technological step is presented in Figure 3.

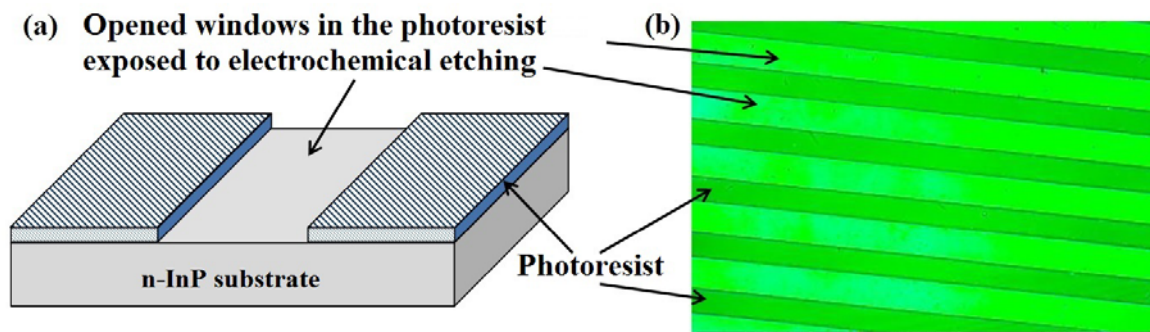


**Figure 3.** (a) Schematic representation of the “C” channel formation via anodization of the semiconductor substrate through opened window in the photoresist. (b) Optical image of developed photoresist after exposure with UV light. The image is from InP surface.

### The choice of the electrolyte.

Usually, the pores in semiconductors are introduced via electrochemical dissolution of materials in electrolytes containing acids such as HF, HCl, H<sub>2</sub>SO<sub>4</sub>, HNO<sub>3</sub> etc. or in alkaline electrolytes. The nature of the electrolyte and its concentration have a strong influence on the morphology of porous layers produced via anodization process.

In the last decade, to make the process of nanofabrication based on electrochemical etching broadly accessible and environmentally friendly, a part of research was focused on nanostructuring in neutral electrolytes. It was proposed and demonstrated using a neutral electrolyte based on an aqueous solution of NaCl instead of commonly used aggressive acids or alkaline electrolytes for the purpose of electrochemical nanostructuring of GaAs and CdSe substrates [24]. Subsequently formation of uniform porous layers and of porous InP membranes was realized for various applications, e.g. nonlithographic manufacturing of semiconductor nanotemplates for the deposition of metal nanotubes [25], and the development of gas sensors was demonstrated [26]. Recently, different porous morphologies produced by anodization in depth of a HVPE-grown GaN substrates with respect to the N- or Ga-face were reported [27].

The results of porosification in neutral electrolyte of III-V and II-VI semiconductor compounds have been reported recently [23].

## Results and discussions

In order to make more channels on the surface of the semiconductor crystal and to investigate the impact of the width of opened regions upon the final distance between the channels in the manufacturing process of the platform, photolithographic masks in the form of strips with a width of 35  $\mu\text{m}$  up to 110  $\mu\text{m}$ , as well as the space between the strips of 35  $\mu\text{m}$  were used (see Figure 3b). This study is motivated by the fact that electrochemical etching starts from the surface unprotected by photoresist (opened windows in photoresist), but once the pores grow with the time ( $t_1$ ), their direction of growth is directed also sideways. Thus, the channel width will be defined not only by the width of the space between the photoresist strips, but also by the electrochemical etching duration, as is shown in Figure 4 for porous region 1. However, with increasing of anodization time up to  $t_2$ , pores in neighboring porous regions 1 meet each other forming an alternating porous layer.

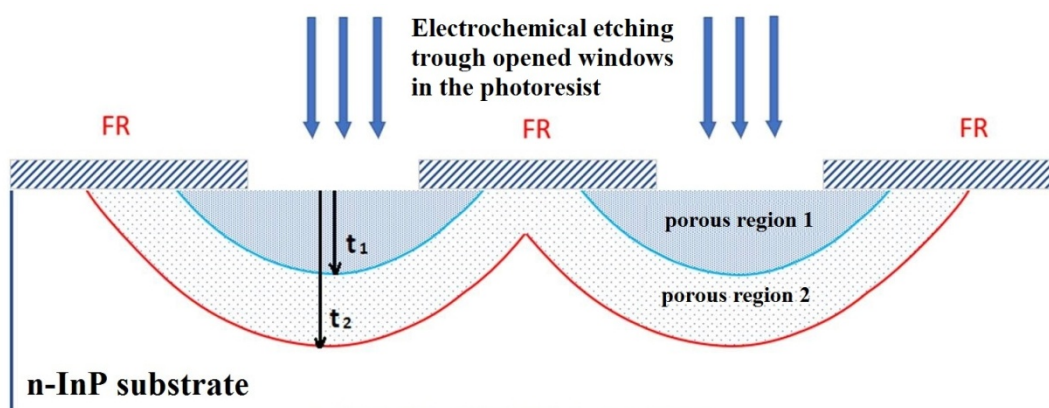


**Figure 4.** Schematic representation of the time evolution of porous layer in depth and under the protected by photoresist regions.

The evolution of the thickness of produced porous layer during anodization is presented in Figure 5. For the purpose of comparison, and to demonstrate that anodization in neutral electrolyte is feasible, the electrochemical etching was performed in two electrolytes, namely HCl and NaCl. It can be seen, that the results of electrochemical etching in NaCl are not much inferior those inherent to etching in HCl. From the morphological point of view, the NaCl electrolyte provides conditions for the growth of crystallographically oriented pores at low applied current densities, passing in arrays of parallel pores in n-InP consisting of current line-oriented pores at higher current densities. It was established that the morphology and the mechanism of pore formation are the same as in the case of anodic etching in HCl electrolyte. Thus, an environmentally-friendly electrolyte based on aqueous solution of NaCl can be used for further exploration of pore formation in InP.

As concern the etch rate, one can see from Figure 5 that it sharply decreases with the duration of anodization. This behavior is quite normal for electrochemical etching and can be explained by difficulties in penetrating of the fresh electrolyte from the surface-electrolyte interface area into pores with diameter of 80 nm. Notwithstanding this, the etch rate is much higher e.g. 32  $\mu\text{m}\cdot\text{min}^{-1}$  for electrochemical etching compared with 4  $\mu\text{m}\cdot\text{min}^{-1}$  in the case of chemical etching.

As was mentioned above, an important technological step consists in optimization of the anodization time for the purpose to stop the electrochemical etching after formation of the porous region 1, see Figure 4.

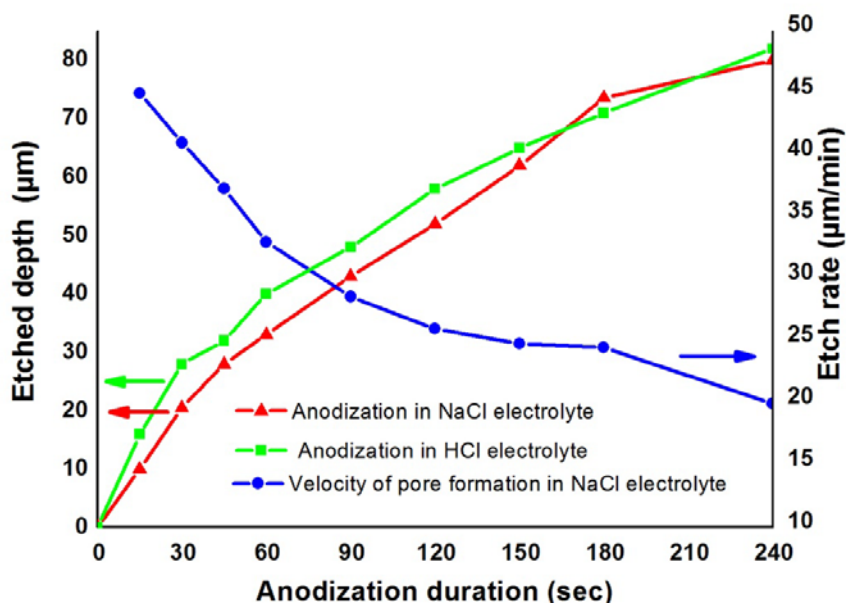


**Figure 5.** Evolution of thickness of porous layer and etch rate of anodized InP crystal in NaCl and HCl electrolyte.

Figure 6a illustrates a SEM image in cross-section and tilted of formed porous channel after 1 min of anodization in NaCl electrolyte.

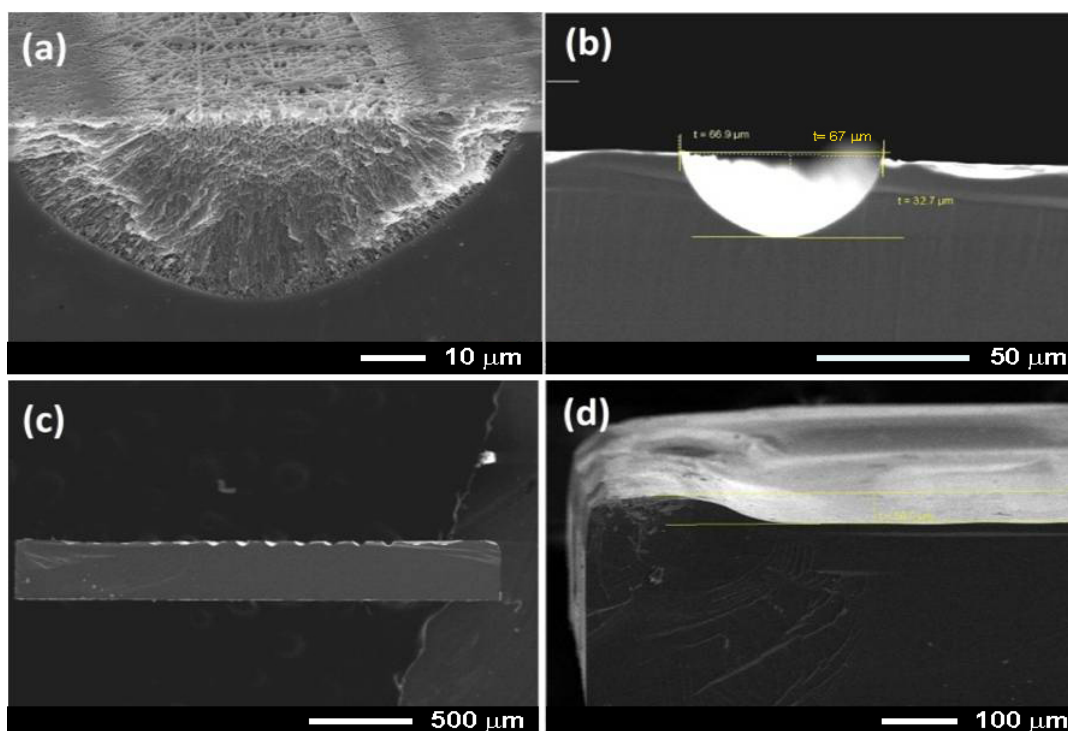


**Figure 6.** SEM images of the n-InP semiconductor substrate: (a) - after electrochemical etching in NaCl electrolyte for 1 min through opened windows in the photoresist; (b) - the semicircular channel obtained after chemical removal of the porous layer from (a); (c) - array of formed parallel channels on the same chip; (d) - after electrochemical etching for 2 min and chemical removal of the porous layer.

It was established that, as a result of anodization through photolithographic mask with strip width of  $110\ \mu\text{m}$  and the distance between them of  $35\ \mu\text{m}$  for duration of 1 min, followed by chemical dissolution of formed porous channel, we obtained a channel with the thickness of  $32\ \mu\text{m}$  and width of  $67\ \mu\text{m}$ , as is shown in Figure 6b.

The width of the formed channel is more than 2 times larger than the width of the initial space between the strips. Respectively, between 2 consecutive channels are not  $110\ \mu\text{m}$ , but  $77\ \mu\text{m}$ . Formation of parallel array of channels on the chip, as is presented in Figure 6c, will allow easier positioning of microtubes on the channel.

Usually, large quantities of micrometer-long nanowires or nanotubes can be obtained on different substrates. However, during the transfer on the chip, their length can be significantly reduced, e.g. via ultrasonic bath used to detach the nanotubes from the growth substrate. In the Table 1 we present the data regarding the width of opened windows in the photoresist and expected width of the resulted "C" shaped channel after electrochemical etching for 1 min in NaCl electrolyte.

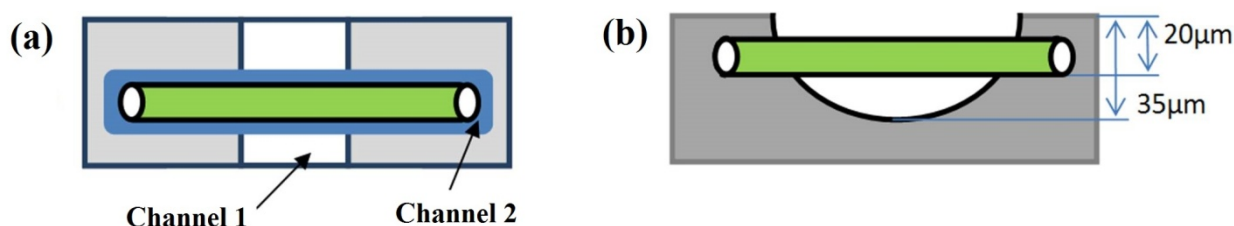
At a longer duration of electrochemical etching, the formed porous layer schematically represented in Figure 4 as the porous region 2, merges with the neighboring porous region, and after removal of the formed porous layers a large etch pit will be obtained (see Figure 6d) instead of a flat surface with array of channels presented in Figure 6c.

Table 1

**Correlation between width of opened windows in the photoresist and expected width of the "C" shaped channel.**

1 min etching of n-InP in 3.5 M NaCl at applied voltage 5V				
Width of opened windows in the photoresist, $\mu\text{m}$	10	35	70	100
Width of the resulted "C" shaped channel, $\mu\text{m}$	45	70	105	135

The following suggestion could be added to the technological process as a possible but not mandatory optimization. It is proposed to place the investigated microtube in a specially-created channel oriented perpendicular to channel 1, as it is shown in Figure 7a. For the formation of channel 2 an additional photolithographic process will be involved as well as an additional electrochemical etching for 30 sec which will result in the deepening of the channel at about  $20\ \mu\text{m}$  from the surface. The need in this channel 2 is motivated by the fact that the microtube will be deepened in the platform (see Figure 7b) and will have a higher stability than on the flat surface (especially under application of the mechanical stresses).



**Figure 7.** (a) Schematic representation in top view and cross-section view in (b) of the optimized platform.



## Conclusions

We elaborated the design of the platform for the study of flexoelectric properties of GaN microtubes with the diameter of 2-5  $\mu\text{m}$  and the wall thickness of 50 nm. The technological process was optimized experimentally, namely: the optimal width of the photolithographic mask strips, the space between them and the duration of the electrochemical etching were determined. It was proposed to introduce a perpendicular channel in which the microtube will be placed to reach a higher stability on the platform during the measurements. It was demonstrated that electrochemical etching in NaCl and HCl electrolytes differs not much from each other. Thus, the environmentally-friendly electrolyte based on aqueous solution of NaCl can be used for further exploration of pore formation in InP.

## Acknowledgements

This research was funded by Ministry of Education, Culture and Research of Moldova under the project no. 20.80009.5007.20.

## References

1. Ma W., Cross L.E. Flexoelectric Polarization in Barium Strontium Titanate in the Paraelectric State. In: *Appl. Phys. Lett.*, 2002, 81 (19), pp. 3440–3442.
2. Ma W., Cross L. E. Strain-Gradient-Induced Electric Polarization in Lead Zirconate Titanate Ceramics. In: *Appl. Phys. Lett.*, 2003, 82 (19), pp. 3293–3295.
3. Wang B., Gu Y., Zhang S., Chen L-Q. Flexoelectricity in solids: Progress, challenges, and perspectives. In: *Progress in Materials Science*, 2019, 106, 100570.
4. Baskaran S., He X., Wang Y., Fu J.Y. Strain Gradient Induced Electric Polarization in  $\alpha$ -Phase Polyvinylidene Fluoride Films Under Bending Conditions. In: *J. Appl. Phys.*, 2012, 111 (1), 014109.
5. Chu B., Salem D.R. Flexoelectricity in Several Thermoplastic and Thermosetting Polymers. In: *Appl. Phys. Lett.*, 2012, 101 (10), 103905.
6. Meyer R.B. Piezoelectric Effects in Liquid Crystals. In: *Phys. Rev. Lett.*, 1969, 22 (18), p. 918.
7. Deng Q., Liu L., Sharma P. Flexoelectricity in Soft Materials and Biological Membranes. In: *J. Mech. Phys. Solids*, 2014, 62, pp. 209–227.
8. Ahmadpoor F., Deng Q., LIU L., Sharma P. Apparent Flexoelectricity in Lipid Bilayer Membranes Due to External Charge and Dipolar Distributions. In: *Phys. Rev. E*, 2013, 88 (5), 050701.
9. Mohammadi P., Liu L., Sharma P. A Theory of Flexoelectric Membranes and Effective Properties of Heterogeneous Membranes. In: *ASME J. Appl. Mech.*, 2014, 81 (1), 011007.
10. Kogan S.M. Piezoelectric effect during inhomogeneous deformation and acoustic scattering of carriers in crystals. In: *Sov. Phys. Solid State*, 1964, 5, pp. 2069–2070.
11. Bursian E. Zaikovskii O. I. Changes in curvature of ferroelectric film due to polarization. In: *Sov. Phys. Solid State*, 1968, 10, pp. 1121–1124.
12. Tagantsev A.K. Piezoelectricity and flexoelectricity in crystalline dielectrics. In: *Phys. Rev. B*, 1986, 34, pp. 5883–5889.
13. Zubko P., Catalan G. Tagantsev A.K. Flexoelectric effect in solids. In: *Annu. Rev. Mater. Res.*, 2013, 43, pp. 387–421.
14. Majdoub M.S., Sharma P. Cagin T. Enhanced size-dependent piezoelectricity and elasticity in nanostructures due to the flexoelectric effect. In: *Phys. Rev. B*, 2008, 77, 125424.
15. Lee D., Yoon A., Jang S.Y., Yoon J.-G., J.-S. Chung M. Kim J. F. Scott T. W. Noh. Giant flexoelectric effect in ferroelectric epitaxial thin films. In: *Phys. Rev. Lett.* 2011, 107, 057602.
16. Lu H., Bark C.-W., Esque De Los Ojos D., Alcala J., Eom C. B., Catalan G., Gruverman A. Mechanical writing of ferroelectric polarization. In: *Science*, 2012, 336, pp. 59–61.
17. Bhaskar U.K., Banerjee N., Abdollahi A., Wang Z., Schlom D.G., Rijnders G., Catalan G. A flexoelectric microelectromechanical system on silicon. In: *Nat. Nanotechnol.*, 2016, 11, pp. 263–266.
18. Karanassios V., Mew G. Anisotropic Wet Chemical Etching of Si for Chemical Analysis Applications. In: *Sensors and Materials*, 1997, 9 (7), pp. 395-416.

19. Seidel H., Csepregi L., Heuberger A., Baumgartel H. Anisotropic etching of crystalline silicon in alkaline solutions I. Orientation dependence and behavior of passivation layers. In: *J. Electrochem. Soc.* 1990, 137, pp. 3612–3626.
20. Kim B., Cho D. Aqueous KOH etching of silicon (110). In: *J. Electrochem. Soc.*, 1998, 145, pp. 2499–2508.
21. Shikida M., Tokoro K., Sato K., Uchikawa D. Differences in anisotropic etching properties of KOH and TMAH solutions. In: *Sensors Actuators A*, 2000, 80, pp. 179–188.
22. Gosalvez M., Zubel I., Viinikka E. Handbook of Silicon Based MEMS Materials and Technologies. ed V Lindroos Part IV ch 24 (New York: Elsevier) pp. 375–407, 2010.
23. Monaico E., Tiginyanu I., Ursaki V. Porous semiconductor compounds. In: *Semiconductor Science and Technology*, 2020, 35, 103001.
24. Tiginyanu I.M., Ursaki V.V., Monaico E., Foca E., Föll H. Pore Etching in III-V and II-VI Semiconductor Compounds in Neutral Electrolyte. In: *Electrochem. Solid-State Lett.*, 2007, 10 (11), pp. D127-D129.
25. Tiginyanu I.M., Monaico E., Albu S., Ursaki V.V. Environmentally friendly approach for nonlithographic nanostructuring of materials. In: *Phys. Stat. Sol. (RRL)*, 2007, 1 (3), pp. 98–100.
26. Volciuc O., Monaico E., Enachi M., Ursaki V.V., Pavlidis D., Popa V., Tiginyanu I.M. Morphology, luminescence, and electrical resistance response to H<sub>2</sub> and CO gas exposure of porous InP membranes prepared by electrochemistry in a neutral electrolyte. In: *Applied Surface Science*. 257 (3), pp. 827-831.
27. Monaico Ed., Moise C., Mihai G., Ursaki V. V., Leistner K., Tiginyanu I M., Enachescu M., Nielsch K. Towards Uniform Electrochemical Porosification of Bulk HVPE-Grown GaN. In: *J. Electrochem. Soc.*, 2019, 166, H3159-3166.